The Application of Electrical and Current Signature Analysis for DFIG Turbine and Powertrain Defects

Howard W Penrose, Ph.D., CMRP, CEM, CMVP

President, MotorDoc LLC

Lombard, Illinois, USA

howard@motordoc.com

Abstract—**Electrical and current signature analysis (ESA/MCSA) techniques provide a valuable method for detecting defects in wind turbine generators, particularly in doubly-fed induction generator (DFIG) systems. This paper explores the application of ESA/MCSA in identifying defects such as wye-ring fractures, bearing wear, and gearbox faults. We discuss the data acquisition process, spectral analysis methodologies, and case studies demonstrating ESA/MCSA's effectiveness in real-world turbine diagnostics and prognostics.**

Index Terms—**DFIG, ESA, MCSA, Prognostics, Wind Generators**

I. INTRODUCTION

Electrical Signature Analysis (ESA) and Motor Current Signature Analysis (MCSA) are prognostic techniques widely used in commercial, military, industrial and utility sectors to evaluate the condition of electrical and mechanical components of electric machines. These methods utilize spectral analysis of current and voltage signals to detect abnormalities that reflect electrical and mechanical degradation and faults. Both of these technologies have proven effective in wind power applications, particularly in doubly-fed induction generator (DFIG) turbines, which constitute a majority of the wind energy market. The ability to detect component-specific faults such as generator rotor issues, gearbox wear, and bearing defects can help mitigate downtime and reduce overall maintenance costs in wind turbine operations.

The use of a combination of voltage and current for ESA was developed by Oak Ridge National Labs in the mid-1980s and patented in 1990.[1] MCSA was initially developed at the Gordon University in Aberdeen, Scotland, in parallel and involved the use of a single phase of current for analysis.[2] ESA was originally developed to analyze bearing and gear wear in motor operated valves while MCSA focused on rotor testing. After 2000 the use of ESA for machine defects and driven equipment defects was furthered by research and by 2003 the first wind generation was evaluated in the Mojave dessert. Researchers also pursued the abilities of MCSA to look beyond the machine rotor and by 2024 methods for evaluating wind generators were established.[3]

The author began research into wind generation analysis using electrical and current signature analysis in 2003. Prognostics associated with stator, rotor and powertrain defects and severity analysis was also initially published in 2010 and 2015[4]. The utilization of ESA as a method for determining the root cause of generator and powertrain fatigue and transformer overheating was published in 2022[5]. In 2024 the ability to utilize current signature analysis for generator and powertrain faults in all types of wind generator platforms was discovered, which is the purpose of this paper, which will focus on DFIG.

Penrose and Alewine discussed the research performed within the wind industry on the ability to detect a variety of generator and powertrain faults. This study reviewed the specific type of DFIG faults including wye-ring rotor failures, which involves the fatigue of the rotor connection which results in fractures and catastrophic failure. The study also identified the variety of powertrain defects that were identified[6].

Within DFIG generators, the common severe failure is related to the rotor connection which involves a fracture in the rotor wye ring. The generator can survive a single fracture but on the second fracture the components may expand resulting in contact with the stator and complete generator failure. If caught early most wye ring failures can be repaired in-place with minimum downtime and expense. The powertrain issues include gearbox gear and bearings, and main bearing defects such as lubrication, wear and electrical discharge. Gearbox and main bearing defects are amongst the longest to repair and the most expensive, having a sizeable impact on a wind turbines return on investment.

Without fault detection it is estimated that during the planned 25-year life of a turbine there will be two generator replacements, one gearbox and two bearing replacements. The ability to repair up-tower for some of the defects reduces cost and downtime while the ability to plan for repairs can reduce outage time considerably. Monitoring data may also be used to determine the fault-drivers and root-causes of each failure as data utilized in a root cause failure analysis.

II. METHODOLOGY

A. Electrical and Current Signature Analysis

The two systems used for this study include an ESA system that gathers three phases of voltage and current at 12 kHz sampling (S_r) and an MCSA system that samples one phase of current at 44.1 kHz. As shown in (1), the result is a resolution (R) of 0.02 Hz for the ESA system over 48 seconds (t) and 0.008 Hz for the MCSA system over 120 seconds.

$$S_r / (t * S_r) = R \tag{1}$$
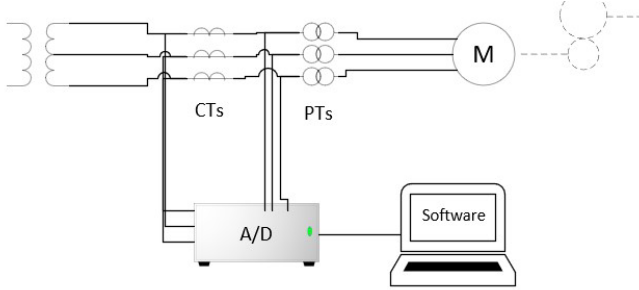
Figure 1: Typical ESA setup with three phases of voltage and current.

The setup of an ESA system is shown in Figure 1 where the data is collected via current transformers and voltage clips or potential transformers. The data is then processed using an analog to digital signal processor and collected by software often through an USB or ethernet. The data is then processed in order to evaluate through spectral analysis and power quality data. In the case of an MCSA system, the current data follows the same process, although normally results in spectral analysis only.

B. Data Processing and Analysis

ESA and MCSA utilize the magnetic field in the air gap between the rotor and stator, influenced by different effects that generate distortions in the current and voltage waveforms. Anomalies and defects can be mathematically modeled resulting in specific frequencies for each component that impacts the magnetic field radially or torsionally. The air gap flux density can be modeled as shown in (2).[7]

$$B_g(\theta) = B_0 \sum_{n=1}^{\infty} \epsilon_n \cos(n\theta + \emptyset_n) \tag{2}$$

Where B_0 is the nominal air gap flux density, ϵ_n represents the magnitude of the n-th harmonic due to defects, Θ is the angular position and ϕ_n is the phase angle of the n-th harmonic. Defects result in a distorted waveform represented as (3) with E_O as the fundamental electro-magnetic force (EMF), and E_n represents the n-th harmonic of the EMF. This results in a distorted current waveform as shown in (4) where I(t) is the current waveform at time increment $Z(\omega)$ and Z represents the impedance of the electric machine.

$$e(t) = E_0 \sin(\omega t + \phi) + \sum_{n=1}^{\infty} E_n \sin(n\omega t + \emptyset_n) \tag{3}$$

$$I(t) = \frac{E(t)}{Z(\omega)} \tag{4}$$

In addition to the radial effects, the torsional effects of electric machine bearings and driven equipment appear as (5). The effect is also in the air gap with g(t) is the effective air gap magnetic field at time t, g_O is the nominal air gap length, γ is the amplitude of the variation, ω_m is the mechanical angular frequency, and ϕ_m is the phase angle of the variation.

$$g(t) = g_0[1 + \gamma \sin(\omega_m t + \phi_m)] \tag{5}$$

The time-varying air gap affects the magnetic linkage, impacting the magnetic fields and current waveform (6) in which $\phi(t)$ is the magnetic linkage at time t, ϕ_O is the nominal flux linkage and γ_n represents the n-th harmonic of the flux variation.

$$\Phi(t) = \Phi_0[1 + \sum_{n=1}^{\infty} \gamma_n \sin(n\omega_m t + \phi_{m,n})] \tag{6}$$

$$\Delta g(\theta, t) = \Delta g_{radial}(\theta) + \Delta g_{torsional}(t) \tag{7}$$

Harmonics are induced into the EMF which affects the current waveform in a similar way as the radial effects. When both radial and torsional conditions exist their combined effects on the magnetic field, voltage and current waveforms are more complex with the overall air gap variations shown as (7) at time t. The combined magnetic field (8) and combined EMF and current waveform include harmonics from torsional and radial conditions (9).

$$B_g(\theta, t) = B_0[1 + \sum_{n=1}^{\infty} \epsilon_n \cos(n\theta + \emptyset_n)$$
$$+ \sum_{m=1}^{\infty} \gamma_m \sin(m\omega_m t + \phi_m)] \tag{8}$$

$$e(t) = E_0 \sin(\omega t + \phi) + \sum_{n=1}^{\infty} E_n \sin(n\omega t + \emptyset_n)$$
$$+ \sum_{m=1}^{\infty} E_m \sin(m\omega_m t + \emptyset_m) \tag{9}$$

In addition, when looking at a complete powertrain as well as the generator, the dampening effects of the components need to be considered. This includes across the coupling, gearbox, and main shaft. As the generator bearings and powertrain components are torque-related, the impact of these compenents have a very small impact.

The line frequency is considered the carrier frequency with conditions shown as amplitude modulated message frequencies. The signals for voltage and current can be shown with m(t) as the message (10). The message is displayed as an FFT with the prominent peak at the carrier, or line, frequency and sidebands of the message signal such that f_c +/- f_m. The spectral data is converted to -dB (11), which results in a non-load dependent spectra.

$$s(t) = (A_c + m(t)) \sin(2\pi f_c t) \qquad (10)$$

$$dB = 20 \log_{10} \left(\frac{I_{fm}}{I_{fc}} \right) \qquad (11)$$

When the frequencies of concern are less than the line (carrier) frequency then they show as sidebands around the carrier frequency. If greater than line frequency then the peaks are +/- the line frequency around the calculated frequency. The values of concern are determined as the decibels down from the peak value of 0dB to a -dB value.

III. GENERATOR CONDITION ANALYSIS

The conditions for review include the transformer, generator, coupling, gearbox, main bearings and shaft, and certain blade conditions. Within the transformer we can see load and harmonic conditions. Generator conditions include the bearings, collector rings, rotor, stator, connections and rotor leads. In the gearbox the technology reviews all bearings and gear conditions. For the main shaft alignment to the gearbox carrier and main bearings. Finally, blade unbalance, alignment, and certain severe conditions.

With MCSA the transformer, power quality and loose connection conditions are unavailable for analysis. In all cases, using spectral analysis of ESA and MCSA, the resolution is necessary in order to separate between bearings, rotor connections, and other peaks which will be within a few fractions of a hertz different.

In this paper we will identify three major conditions including rotor wye ring, stator wedge loss, and a main bearing defect.

A. Rotor Wye Ring Defects

One of the more common issues in DFIG generators that has the potential for catastrophic impact is the rotor wye ring failure (Figure 2). From a final detection standpoint, the current will oscillate at twice the slip frequency which is referred to as the pole pass frequency (PPF). When the defect approaches this point there are hours left before catastrophic failure. The failure is known to be generated as a fatigue failure resulting in fractures that generally break.

When the fractures start there is a change in rotor circuit impedance. This results in an unbalanced rotating magnetic field that emulates a dynamic eccentricity, or magnetic orbit. The PPF (12) and dynamic eccentricity (13) are two of the early indicators in ESA/MCSA. The results show in a spectral analysis as shown in Figure 3.

Figure 2: Failed rotor connection and wye ring failure detected early.
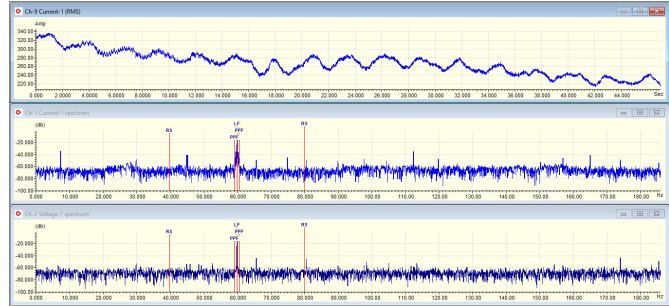
Figure 3: ESA RMS current waveform and voltage and current spectra for a wye ring failure.

$$PPF = P * (LF - RS) \qquad (12)$$

$$Ecc_{DE} = RB * RS \pm [(k * LF) \pm RS] \qquad (13)$$

Where RS is the running speed, in hertz. Where ECC_{DE} are the dynamic eccentricity peaks, RB is the number of rotor bars or slots, and LF is the line frequency in hertz.

B. Stator Wedge Loss

A majority of wind turbine generators use ferrous wedges to reduce air gap harmonics, resulting in improved efficiency, reduced noise and cooler operation. When there is an unbalance in the circuit, such as loose or missing wedges, the signature appears as (14) with any level above the noise floor. The higher the peak the greater the impact or number of wedges, or coil movement.

$$S_{wedge} = (RS * SS) \pm LF \qquad (14)$$

$$S_{winding} = S_{wedge} \pm RS \qquad (15)$$

Where SS is the number of stator slots. A degrading winding condition, such as a developing short, would show as (15) which are running speed sidebands around the stator

frequencies, whether those frequency peaks are present or not. One of the dangers is when the wedges disintegrate in the air gap and the ferrous material drills into the insulation, resulting in a ground (Figure 4 and 5).
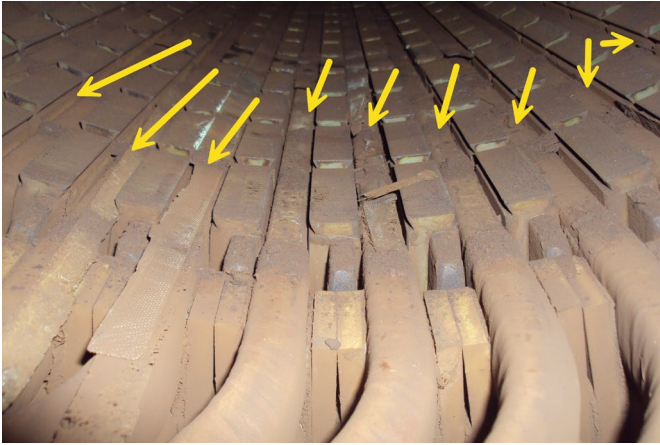
Figure 4: Wind generator stator with missing wedges.
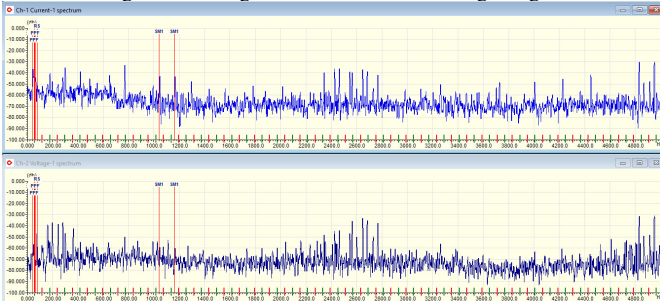
Figure 5: Stator defect, missing wedges.

C. Main Bearing Defect

Main bearing defects are further out on the power train and turn at under 20 RPM. In most DFIG there will normally be two main bearings on the main shaft. The associated frequencies would be based on the speed of the main shaft time multipliers associated with inner race, outer race, cage and rollers. Figure 6 identifies where the peaks are located identifying outer race frequencies that indicate the need for proper greasing techniques.

Figure 6: Peaks associated with bearing conditions with the red arrows showing the outer race frequencies in voltage spectra.

IV. CONCLUSION

Electrical and current signature analysis are powerful prognostic tools for detecting electrical and mechanical conditions through a wind turbine generator and powertrain. The transducer is the magnetic field between the rotor and stator which allows the user to evaluate all of the components in the generator and powertrain at the same time. The resolution of an ESA/MCSA instrument is crucial in separating out conditions, especially in complex systems such as wind power. In general, a resolution of at least 0.01 Hz is required.

REFERENCES

[1] H. Haynes and D. Eissenberg, "Motor Current Signature Analysis Method for Diagnosing Motor Operated Devices," U.S. Patent 4,965,513, Oct. 23, 1990.

[2] W. Thomson and I. Culbert, *Current Signature Analysis for Condition Monitoring of Cage Induction Motors*, New Jersey, IEEE, 2017.

[3] Penrose, H., "The Scope and Application of Electrical Signature Analysis in Windpower," CBM Connect, cbmconnect.com, 2023.

[4] H. W. Penrose, "Insulation system reliability in wind generation," *2015 IEEE Electrical Insulation Conference (EIC)*, Seattle, WA, USA, 2015.

[5] H. W. Penrose, "Evaluation of Asynchronous Wind Generator Stator Magnetic Slot Wedge and Coil Movement Using Electrical Signature Analysis," *2021 IEEE Electrical Insulation Conference (EIC)*, Denver, CO, USA, 2021, pp. 1-4.

[6] K. Alewine and H. Penrose, "Field Experiences Utilizing Electrical Signature Analysis to Detect Winding and Mechanical Problems in Wind Turbine Generators," *2020 IEEE Electrical Insulation Conference (EIC)*, Knoxville, TN, USA, 2020, pp. 246-248.

[7] Penrose, H, "Evaluating Wind Turbines with Electrical Signature Analysis," National Electrical Testing Association Emerging Technologies, Fall 2024, pp. 4-11.